Thermodynamic Stability of a κI Immunoglobulin Light Chain: Relevance to Multiple Myeloma

Connie M. Chung,* Jenny D. Chiu,* Lawreen H. Connors,[†‡] Olga Gursky,* Amareth Lim,[†‡§] Andrew B. Dykstra,[§¶] Juris Liepnieks,[‖] Merrill D. Benson,[‖] Catherine E. Costello,[†‡§] Martha Skinner,[‡] and Mary T. Walsh*[†‡]

*Department of Physiology and Biophysics, [†]Department of Biochemistry, [‡]Amyloid Treatment and Research Program, [§]Mass Spectrometry Resource, [¶]Department of Chemistry, Boston University School of Medicine, Boston, Massachusetts; and [‖]Department of Pathology and Laboratory Medicine, Indiana University School of Medicine, Indianapolis, Indiana

ABSTRACT Immunoglobulin light chains have two similar domains, each with a hydrophobic core surrounded by β-sheet layers, and a highly conserved disulfide bond. Differential scanning calorimetry and circular dichroism were used to study the folding and stability of MM-κI, an Ig LC of κI subtype purified from the urine of a multiple myeloma patient. The complete primary structure of MM-κI was determined by Edman sequence analysis and mass spectrometry. The protein was found to contain a cysteinyl post-translational modification at Cys^{214}. Protein stability and conformation of MM-κI as a function of temperature or denaturant conditions at pH 7.4 and 4.8 were investigated. At pH 4.8, calorimetry demonstrated that MM-κI undergoes an incomplete, cooperative, partially reversible thermal unfolding with increased unfolding temperature and calorimetric enthalpy as compared to pH 7.4. Secondary and tertiary structural analyses provided evidence to support the presence of unfolding intermediates. Chemical denaturation resulted in more extensive protein unfolding. The stability of MM-κI was reduced and protein unfolding was irreversible at pH 4.8, thus suggesting that different pathways are utilized in thermal and chemical unfolding.

INTRODUCTION

Immunoglobulin light chains (Ig LCs) are composed of two separate domains, each containing 100–110 amino acids and having an approximate molecular weight of 12,000. A loosely folded loop region joins the N-terminal variable (V_L) domain to the C-terminal constant (C_L) domain. The V_L and C_L domains have similar tertiary structures, each being composed of two β-sheets and containing a single intrachain disulfide bond. This cysteine is buried within several stretches of nonpolar residues located in the interior hydrophobic core region between the β-sheets (Amzel and Poljak, 1979). The disulfide bond in the hydrophobic core stabilizes the folded conformation of the individual domains, as well as the entire LC molecule.

The existence of partially unfolded intermediates of Igs or Ig fragments, including LCs or their individual domains, was first suggested by Rowe and Tanford (1973). Brody (1997) and others (Tischenko et al., 1982; Büchner et al., 1991; Martsev et al., 1995; Shimba et al., 1995) have reported the existence of unfolding intermediates after exposure of IgG to denaturing detergents, urea, and heat. It was demonstrated that the formation of various intermediates resulted from differences in disulfide bond sensitivity to denaturing agents within the separate Ig domains. The biophysical behavior of an Ig molecule is therefore dependent on the presence of these individual domains (whose structure is determined by amino acid content/sequence) and concomitantly influenced by environmental conditions.

The thermodynamic stability of single- and multidomain proteins can be studied using differential scanning calorimetry (DSC). Parameters obtained from calorimetric measurements include melting temperature (T_m), calorimetric enthalpy (ΔH_{cal}), effective or van't Hoff enthalpy (ΔH_{vH}), and a number of cooperatively unfolding units or domains, which can be assessed by using the ratio $\Delta H_{cal}/\Delta H_{vH}$ (Brandts and Lin, 1990; Privalov and Potehkin, 1986; Sturtevant, 1987). Changes in protein stability and structure (secondary and tertiary) as a function of temperature, denaturant concentration, and/or pH can be studied using far- and near-UV circular dichroism (CD) analyses (Fasman, 1996). CD can provide thermodynamic information, including unfolding temperature, van't Hoff enthalpy, and free energy of unfolding under a variety of environmental conditions.

The structural stability of an Ig LC protein (MM-κI), isolated from the urine of an individual with multiple myeloma and characterized as a member of the κI subtype, was investigated. The protein was studied at pH 7.4 and 4.8 using DSC and far- and near-UV CD. The solution composition and pH values were chosen to model two physiological environments in which LCs are found, i.e., the plasma compartment (pH 7.4), where LCs are normally soluble, and the nephron (pH 4.8), where LCs may either be soluble or in a pathologically deposited form depending on amino acid composition and physiological parameters. Determining the effects of environmental factors on LC conformational

Submitted February 14, 2005, and accepted for publication March 18, 2005.

Dr. Mary T. Walsh died August 16, 2004.

Address reprint requests to Lawreen H. Connors, Dept. of Biochemistry, Boston University School of Medicine, 715 Albany St., K-507, Boston, MA 02118-2526. Tel.: 617-638-4313; E-mail: lconnors@bu.edu.

0006-3495/05/06/4232/11 $2.00

doi: 10.1529/biophysj.105.061317

changes is key to understanding the mechanisms of disease in Ig LC pathologies such as multiple myeloma and primary amyloidosis.

METHODS

Protein purification and sequence analysis

MM-κI was purified from the urine obtained on an individual with multiple myeloma who did not have amyloidosis or cast nephropathy. It is not known whether the patient had developed Acquired Fanconi syndrome, which may sometimes be associated with multiple myeloma. The urine was dialyzed against deionized water in 6–8 kDa molecular weight cutoff dialysis tubing (Spectrapor, Spectrum Laboratories, Rancho Domingues, CA) and lyophilized. Protein was reconstituted in 20 mM sodium phosphate buffer, pH 7.1 and passed through an Affi-gel Blue column (Bio-Rad, Hercules, CA) to remove albumin. The albumin-free protein sample was dialyzed against water, lyophilized, and reconstituted in the appropriate buffer for biophysical studies. Purity was assessed by SDS-PAGE on 10–15% gradient gels using the PhastSystem (Amersham-Pharmacia Biotech, Piscataway, NJ) (Laemmli, 1970). Samples were electrophoresced with and without β-mercaptoethanol and visualized using Coomassie blue and/or silver stain. Immunodetection of proteins transferred to Immobilon-P was performed using polyclonal rabbit anti-human LC-κ antibodies (Sigma, St. Louis, MO), alkaline phosphatase-linked goat anti-rabbit IgG (Promega, Madison, WI), and 5-bromo-4-chloro-3-indolyl-phosphate/nitor blue tetrazolium phosphatase substrate (Kirkegaard & Perry Laboratories, Gaithersburg, MD) (Towbin et al., 1979). Isoelectric focusing was performed on the Pharmacia PhastSystem using pH 3–9 Phast IEF gels, broad pI markers (Amersham-Pharmacia Biotech), and Coomassie Blue R-350 for detection. Protein concentration was assessed by the method of Lowry et al. (1951). Biophysical studies were performed in phosphate buffered saline (PBS, 50 mM potassium phosphate, 0.15 M sodium chloride) at pH 7.4 or 4.8 with or without varying concentrations of guanidine-HCl (GuHCl).

The complete amino acid sequence of MM-κI was determined by a combination of direct N-terminal sequencing and peptide-mapping methods. N-terminal sequence analysis was performed on an Applied Biosystems Model 473A protein sequencer (Applied Biosystems, Foster City, CA) (Wally et al., 1999). Tryptic peptides of reduced and alkylated MM-κI were produced, purified on a Beckman Ultrasphere ODS HPLC column (Beckman Coulter, Fullerton, CA), and sequenced (Dwulet et al., 1985). Mass spectrometry (MS) was used to determine the molecular weight of the intact protein, confirm the amino acid sequence of MM-κI, and identify post-translational modifications of the protein as described previously (Green et al., 1990; Loo et al., 1993; Lim et al., 2001). Briefly, the molecular mass of the intact protein before and after treatment with dithiothreitol was determined using a Micromass Quattro II electrospray ionization (ESI) triple quadrupole mass spectrometer (Beverly, MA). Matrix-assisted laser desorption/ionization (MALDI) mass spectrometric analyses of peptides generated by treatment with trypsin or lysyl endopeptidase Lys-C were performed on a Finnigan MAT Vision 2000 MALDI time-of-flight mass spectrometer (Thermo Electron, San Jose, CA) in the linear mode with delayed extraction (Lim et al., 2001) using 2,5-dihydroxybenzoic acid as the matrix.

Differential scanning calorimetry

Calorimetry was performed on an upgraded MC-2 calorimeter (MicroCal, Northampton, MA) (Walsh and Atkinson, 1990). Samples were dialyzed at 4°C against the appropriate buffer and degassed. Experiments were performed using MM-κI at protein concentrations between 0.46 and 1.73 mg/ml.

Heat capacity measurements were obtained from 5 to 100°C at a rate of 90°C/h under nitrogen gas (20 psi) and each sample was heated/cooled 2–4 times. For each experiment, the buffer baseline was subtracted and the data were normalized to protein concentration. The molecular weight of MM-κI used for molar quantity calculations was 23,514 as determined by ESI mass spectrometry. Thermodynamic analysis of $C_p(T)$ data was performed utilizing ORIGIN software (Freire and Biltonen, 1978; Rigell et al., 1985). The T_m for a transition was the temperature of maximum excess heat capacity. The ΔH_{cal} was calculated from the area under each calorimetric peak. Numerical integration of peaks and resolution of overlapping peaks were performed using linear (Krishnan and Brandts, 1978) or sigmoidal baselines (Fukada et al., 1983). The ratio of the calorimetric to the van't Hoff enthalpy was calculated using the equation $\Delta H_{cal}/\Delta H_{vH} = \Delta H_{cal}^2/C_{p,max}\,4RT_m^2$, where $C_{p,max}$ is the maximum in the heat-capacity function and R is equal to 1.987 cal/deg-mol (Biltonen and Freire, 1978; Privalov and Khechinashvili, 1974). The ratio is equal to 1 for two-state transitions, >1 if transitions are more than two-state and involve unfolding intermediates, and <1 if the cooperatively unfolding unit contains more than one protein molecule (e.g., in the case of self-association) (Privalov and Potehkin, 1986).

Circular dichroism spectroscopy

Circular dichroism studies were performed on an Aviv 62DS spectropolarimeter (AVIV Associates, Lakewood, NJ) (Chung et al., 2001) equipped with a thermoelectric temperature controller. Experiments were performed multiple times on two separate samples. Far-UV spectra (190–250 nm) were recorded in PBS (pH 7.4 or 4.8) at several constant temperatures for thermal stability studies or at 25°C in varying concentrations of GuHCl for denaturant stability investigations. Five to 20 spectra were recorded at 0.5-nm intervals with a bandwidth of 1 nm and an averaging time of 2–10 s. For far- and near-UV CD melts, ellipticity was monitored at constant wavelength while heating at a controlled rate. Near-UV CD spectra (250–320 nm) were recorded in PBS (pH 7.4 or 4.8) at 25°C before and after melts.

Thermal unfolding

Samples were equilibrated for 30 min at each temperature before recording CD spectra at 25, 35, 45, 50, 55, 65, and 75°C, and again at 25°C after cooling. Multiple spectra were recorded, averaged, and corrected for the buffer baseline. Molar residue ellipticity $[\theta]$ values were calculated according to the equation $[\theta](\text{deg-cm}^2/\text{decimol}) = [\theta\ (\text{MRW})]/(10\ \text{l c})$, where θ is the measured ellipticity (millidegrees), MRW is the mean residue weight of the protein amino acids (g/mol), l is the pathlength of the cell (cm), and c is the protein concentration (g/ml) (Greenfield and Fasman, 1969; Walsh et al., 1990).

Thermal melts were corrected for the baseline recorded at 250 nm (far-UV) or 320 nm (near-UV). For far-UV melts, ellipticity was monitored at 250 (baseline), 217 (β-sheet), and 202 nm (random coil) from 5 to 95°C every 0.5°C with an averaging time of 60 s, at protein concentrations of 0.20–0.40 mg/ml in 0.02- or 0.05-cm cells. For near-UV melts, ellipticity was monitored at 320 nm (baseline), 295 and 290 nm (tryptophan), 280 nm (tyrosine), and 260 nm (phenylalanine and disulfide bonds) from 5 to 80°C every 0.5°C with an averaging time of 90 s at protein concentrations of 3–20 mg/ml in 0.1- or 0.2-cm cells. Spectra were recorded at 5 or 25°C before and after melts to assess reversibility.

At 217 nm, thermal melts were analyzed according to methods described by Pace et al. (1989) assuming a two-state unfolding mechanism in which $f_F + f_U = 1$, where f_F and f_U represent the fraction of protein in the folded and unfolded states, respectively. The observed value of θ at any point is $\theta = \theta_F f_F + \theta_U f_U$, where θ_F and θ_U are the values of θ in the folded and unfolded states, respectively. Thus, $f_U = (\theta_F - \theta)/(\theta_F - \theta_U)$. The apparent equilibrium constant (K) and the free energy change (ΔG) were calculated from the equations $K = f_U/(1 - f_U) = f_U/f_F = (\theta_F - \theta)/(\theta - \theta_U)$ and $\Delta G = -RT\ln K = -RT\ln[(\theta_F - \theta)/(\theta - \theta_U)]$.

Values of θ_F and θ_U were obtained by a least-squares fit of the pre- and post-transition baselines.

Chemical denaturation

Denaturant stability was monitored by methods described (Pace, 1986; Pace et al., 1989; Santoro and Bolen, 1992). Stock solutions of PBS buffer (pH 7.4 or 4.8) with and without saturating concentrations of GuHCl were prepared. The refractive index of these solutions was measured using an AO ABBE Refractometer model 104501 (Leica, Buffalo, NY). The molarities of the GuHCl stock solutions were calculated using the equation Molarity = $(57.147\Delta N) + (38.68\Delta N)^2 - (91.60\Delta N)^3$, where N_G is the refractive index of the GuHCl solution, N_B is the refractive index of the buffer, and $\Delta N = N_G - N_B$.

One-half-milliliter samples were prepared containing 0.4 mg/ml MM-κI in PBS (pH 7.4 or 4.8) with 0–6 M GuHCl. The appropriate volume of stock MM-κI (12.9 mg/ml MM-κI in PBS at pH 7.4 or 10.9 mg/ml MM-κI in PBS at pH 4.8) was added to reach a final protein concentration of 0.4 mg/ml. The appropriate volume of GuHCl stock solution (7.29 M in PBS, pH 7.4 and 6.65 M in PBS, pH 4.8) was added to reach the desired concentration of GuHCl. PBS (pH 7.4 or 4.8) was added to reach a total volume of 0.5 ml. GuHCl reference solutions (no MM-κI) were prepared for CD blank solutions by substituting PBS for protein. Protein samples were equilibrated in GuHCl overnight at room temperature. Far-UV spectra were recorded at 25°C in 0.05-, 0.1-, or 0.2-cm cells. Five to 20 scans from 250 to 195 or 205 nm were recorded for each sample and blank, with a 1-nm bandwidth, a 1-nm increment, and an averaging time of 10 s. Reversibility of denaturant-induced unfolding was tested by dilution. Samples in 1.4 M GuHCl were diluted to 0.5 M GuHCl with PBS and incubated at room temperature for two weeks before measuring their spectra.

PBS at pH 7.4 was titrated with HCl (1 N) to acidic pHs and with NaOH (1 or 10 N) to basic pH values. A series of 400 μl samples at pH from ~1 to 12 were prepared by dilution of a stock solution of MM-κI (15.0 mg/ml) to 0.4 mg/ml with PBS at the selected pH. Samples were incubated at room temperature for 24 h and pH was measured before recording far-UV spectra at 25°C. The sample pHs were 1.1, 2.1, 3.1, 4.0, 4.8, 5.6, 6.2, 7.4, 8.1, 9.1, 10.0, 11.2, and 12.1. Reversibility of unfolding was monitored by recording spectra of samples titrated from pH 1, 4, or 11.2–7.4 after incubation at 25°C for 24 h.

RESULTS AND DISCUSSION

SDS-PAGE, Western blotting, and IEF indicated that MM-κI is a 25,000 Da, monomeric LC of the Ig-κ class with a pI from 5.20 to 5.85 (data not shown). The LC was further characterized as a κI protein based on primary structure data obtained by conventional sequence analysis and mass spectrometry (Figs. 1 and 2). Direct sequence analysis of the N-terminus of MM-κI yielded the first 50 residues of the LC not including residues 1 (Asp) and 23 (Cys). The entire primary structure was further determined by conventional sequencing of the tryptic peptides with the exception of residues 108, 143–145, and 212–214.

ESI MS was used to confirm the sequence analysis of MM-κI (Fig. 1). The observed mass of 23,514 ± 2 Da (Fig. 1 *A*) was not consistent with the calculated mass of 23,395 Da obtained using the MM-κI V_L conventional sequence data and the published structure of the κ-C_L domain (Hieter et al., 1980). The calculated mass assumed that two disulfide bonds were present, Cys^{23}–Cys^{88} and Cys^{134}–Cys^{194}. Treatment of the protein with dithiothreitol yielded an observed mass of 23,398 ± 2 Da (Fig. 1 *B*). The 116-Da mass difference between the reduced and nonreduced forms of MM-κI was the result of two internal disulfide bonds and *S*-cysteinylation at Cys^{214}. Interestingly, although *S*-cysteinylation of Cys^{214} has also been reported in an amyloidogenic κI LC (Lim et al., 2001), the frequency of this post-translational modification in LC proteins is not known. Further peptide mapping of MM-κI by MALDI MS gave complete amino acid sequence coverage (Fig. 2) and confirmed the presence of three disulfide bonds in the protein, Cys^{23}–Cys^{88}, Cys^{134}–Cys^{194}, and Cys^{214}–Cys (data not shown). Detection of the ion at *m/z* 931.5 (calculated $[M+H]^+$ *m/z* 932.0) in the lysyl endopeptidase Lys-C digest (Lim, et al., 2001) confirmed the presence of *S*-cysteinylation at Cys^{214}. This protonated molecule corresponded to the Lys-C peptide containing residues 208–214 disulfide-linked to cysteine.

Calorimetry was used to measure thermodynamic values associated with the stability, cooperativity, and reversibility of thermal unfolding of MM-κI. Fig. 3 represents typical endotherms for MM-κI at pH 7.4 (Fig. 3, *A* and *C*) and pH

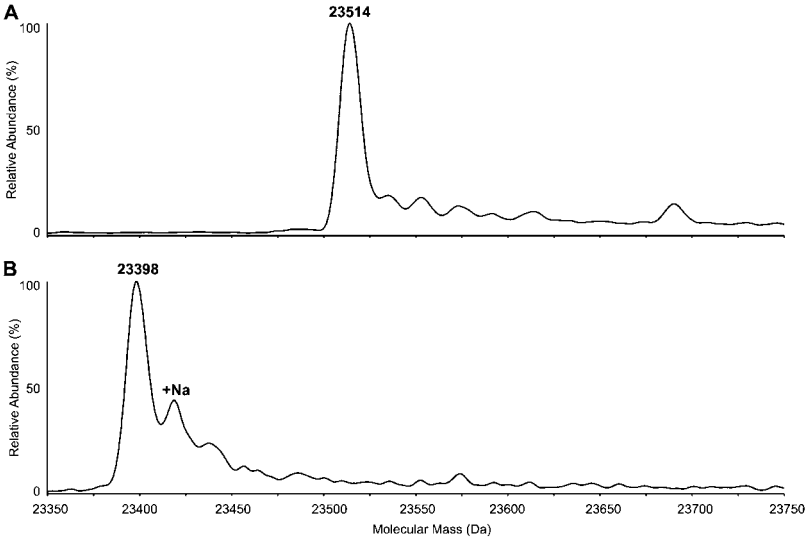

FIGURE 1 The deconvoluted ESI mass spectra of MM-κI (*A*) before and (*B*) after treatment of MM-κI with dithiothreitol.

D	I	Q	M	T	Q	S	P	S	S	L	S	A	S	V	G	D	R	V	T	I	T	C	Q	A	25
S	Q	D	I	I	N	Y	V	N	W	Y	Q	Q	K	P	G	K	A	P	K	V	L	V	Y	D	50
A	S	K	L	E	T	G	V	P	S	R	F	S	G	S	G	S	G	T	D	F	T	F	T	I	75
S	S	L	Q	P	E	D	I	A	T	Y	Y	C	Q	Q	Y	E	N	L	P	L	T	F	G	G	100
G	T	K	V	E	I	K	R	T	V	A	A	P	S	V	F	I	F	P	P	S	D	E	Q	L	125
K	S	G	T	A	S	V	V	C	L	L	N	N	F	Y	P	R	E	A	K	V	Q	W	K	V	150
D	N	A	L	Q	S	G	N	S	Q	E	S	V	T	E	Q	D	S	K	D	S	T	Y	S	L	175
S	S	T	L	T	L	S	K	A	D	Y	E	K	H	K	V	Y	A	C	E	V	T	H	Q	G	200
L	S	S	P	V	T	K	S	F	N	R	G	E	C												214

FIGURE 2 The amino acid sequence of MM-κI. Residues 1–107 were identified by direct sequencing of the first 50 N-terminal residues and analysis of tryptic peptides. Amino acids 108–214 were assigned by analyses of tryptic peptides and comparison to the germline κ-constant region sequence (Hieter et al., 1980) with the exceptions of residues 108, 143–145, and 212–214. The complete sequence, including the post-translational cysteinylation at Cys^{214}, was determined using mass spectrometry.

4.8 (Fig. 3, *B* and *D*). Two consecutive heating scans at each pH, scan 1 and 2, are shown in Fig. 3, *A* and *B*. Scan 1 at each pH was further analyzed after baseline correction, normalization to protein concentration, and curve fitting to a non-two-state model with a single transition (Fig. 3, *C* and *D*). The rugged line represents actual recorded data, and ''best fit'' computer-generated data is presented as a smooth trace. The thermodynamic parameters determined for scan 1 at each pH are presented in Table 1.

The thermal unfolding of MM-κI from 5 to 100°C at pH 7.4 or 4.8 was characterized by a single cooperative partially reversible transition. At pH 7.4, $T_m = 50.2$°C and $\Delta H_{cal} = 36.8$ kcal/mol, whereas at pH 4.8, $T_m = 54.3$°C and $\Delta H_{cal} = 44.5$ kcal/mol. The observed enthalpy changes are significantly smaller than the enthalpy of unfolding for similar-size globular proteins (Pace et al., 1989). This suggests that there is incomplete thermal unfolding of MM-κI, a result that was also consistent with the CD analyses (detailed below). The T_m and ΔH_{cal} for MM-κ_I are greater at pH 4.8 than at pH 7.4, suggesting that the thermal stability of LC at 25°C is higher at pH 4.8. The calorimetric enthalpies for MM-κ_I at pH 7.4 and 4.8 comprise only a fraction of the van't Hoff enthalpies. The ratios of $\Delta H_{cal}/\Delta H_{vH}$ are 0.27 at pH 7.4 and 0.37 at pH 4.8, suggesting that the cooperativity unit at either pH may involve protein oligomers comprised of 2–3 molecules. It is important to note that the transition temperature and enthalpy were independent of the protein concentration (0.46–1.73 mg/ml) in the pH range explored. This suggests that the degree of protein self-association does not significantly change in thermal transition, and hence protein aggregation does not have a large effect on the thermodynamic parameters such as T_m determined in this work.

Far-UV CD was used to study the secondary structure of MM-κI at pH 7.4 and 4.8 as a function of temperature. Fig. 4, *A* and *B*, represent far-UV CD spectra of MM-κI with indicated temperatures at pH 7.4 and 4.8, respectively. At pH 7.4 (25 and 35°C), MM-κI exhibits far-UV CD spectra typical of a predominantly β-sheet protein with negative minima at

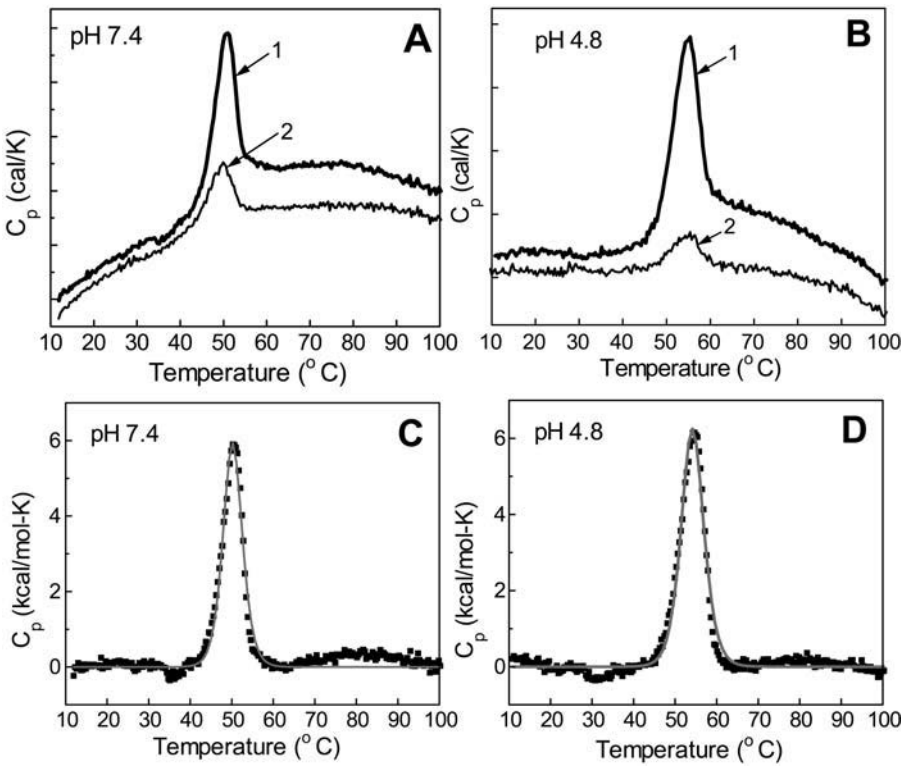

FIGURE 3 Heat capacity function of MM-κI measured by differential scanning calorimetry in two consecutive heating scans, Scan 1 and 2, at (*A*) pH 7.4 and (*B*) pH 4.8 corrected for buffer baseline only. Deconvolution of the heat capacity function at (*C*) pH 7.4 and (*D*) pH 4.8 corrected for heating rate (90°/h), buffer baseline, and protein concentration (1.70 and 1.73 mg/ml, respectively). Actual recorded and best-fit computer-generated data are shown in rugged and smooth lines, respectively.

TABLE 1 Summary of thermodynamic values for MM-κI

	pH 7.4	pH 4.8
Calorimetry		
T_m, °C	50.2	54.3
ΔH_{cal}, kcal/mol	36.8	44.5
ΔH_{vH}, kcal/mol	135	120
$\Delta H_{cal}/\Delta H_{vH}$	0.27	0.37
Far-UV CD		
$T_{1/2}$, °C* 217 nm	45.8	50.4
202 nm	47.6	51.4
T_m, °C†	47.4	48.8
ΔH_{vH}‡	119	159
Near-UV CD		
$T_{1/2}$, °C† 295 nm	49.7	50.2
290 nm	49.7	50.2
280 nm	49.8	50.2
260 nm	50.2	72.0
GuHCl		
$C_{1/2}$, M§	2.90	0.75
$\Delta G_{25°C}$,¶ kcal/mol	5.77	—‖

*Temperature at the midpoint of the unfolding curve.
†Calculated according to Pace (1986) using the data from the insets of Fig. 4, *A* and *B*, $[\theta]_{217\ nm}$ against temperature.
‡Calculated according to Pace et al. (1989) using the data from the insets of Fig. 4, *A* and *B*, $[\theta]_{217\ nm}$ against temperature.
§Concentration of GuHCl at the midpoint of the unfolding transition.
¶Free energy change of unfolding in the absence of GuHCl at 25°C, kcal/mol.
‖Not calculated due to the inability to reliably estimate the pretransition baseline.

217 nm. Over the range from 250 to 215 nm, the spectrum recorded at 45°C is similar to those recorded at 25 and 35°C. However, the minimum shifts to 210 nm with a small increase in negative ellipticity, indicating that some of the β-sheet has converted to random coil. At 50°C, the spectrum is altered further with an additional increase in negative ellipticity and a deeper trough below 210 nm, suggesting further β-sheet unfolding. This trend continues at 55, 65, and 75°C with the spectra at 65 and 75°C being virtually identical. These data imply that all susceptible regions of β-sheet have been converted to random coil by 65°C. At high temperatures, the residual ellipticity at 202 nm is ~−5000 deg-cm^2/dmol (as compared to values of at least −10,000 deg-cm^2/dmol^{-1} characteristic of fully unfolded proteins). This indicates that, upon completion of the thermal unfolding transition at 65–75°C, MM-κI retains a substantial amount of ordered secondary structure. As mentioned previously, these data are consistent with the DSC measurements that yield low ΔH_{cal} and suggest that there is incomplete thermal unfolding of MM-κI. Furthermore, far-UV CD spectra recorded at 25°C before (−) and after (*) heating are similar over the range from 250 to 215 nm, indicating that there is a largely reversible unfolding transition.

At pH 4.8, spectra at 25 to 45°C are similar and typical of a β-sheet protein. At 50°C, the altered spectrum indicates that unfolding has begun. Spectra recorded at 55–75°C are superimposable and typical of a predominantly random coil protein that retains a significant amount of ordered secondary structure. In contrast to the results obtained at pH 7.4, cooling and overnight incubation at 25°C and pH 4.8 does not result in refolded MM-κI. Rather, the spectrum more closely resembles that of a classical random coil protein with the ellipticity at 202 nm further reduced and approaching (but not quite reaching) the value characteristic of 100% random coil. Thus, in contrast to pH 7.4, thermal unfolding at pH 4.8 appears irreversible.

Thermal unfolding data monitoring temperature-dependent changes in β-sheet and random coil in MM-κI were continuously measured at 217 and 202 nm and are presented

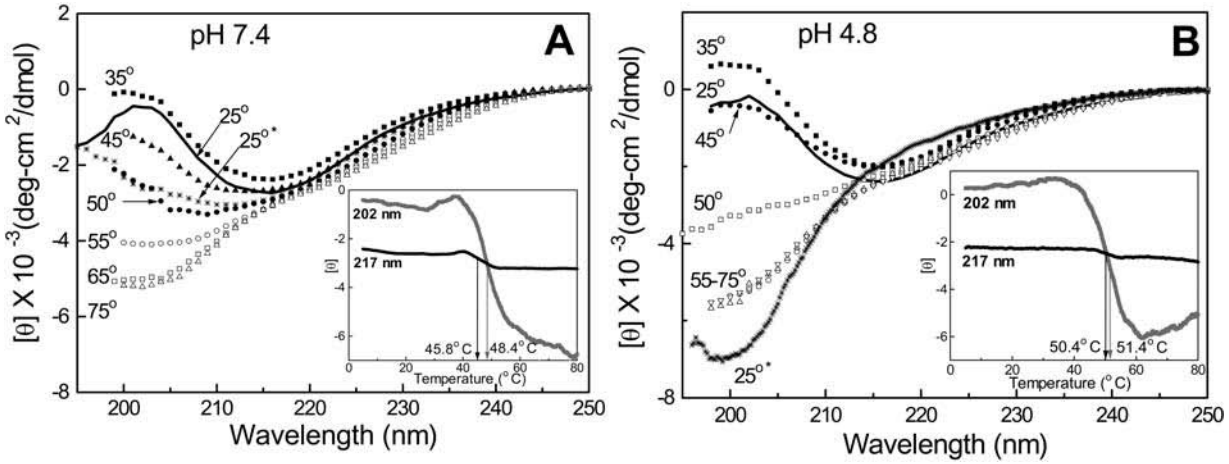

FIGURE 4 Far-UV CD spectra of MM-κI in PBS. Thermal stability analysis at (*A*) pH 7.4 and (*B*) pH 4.8 with spectra recorded at 25, 35, 45, 50, 55, 65, and 75°C after 30-min equilibration at each temperature. Samples were cooled from 75 to 25°C, incubated at 25°C overnight, and spectra were recorded at 25°*C. Insets show thermal unfolding of MM-κI in PBS at pH 7.4 and pH 4.8. Samples were monitored at 217 nm (*solid line*) and 202 nm (*shaded line*). Ellipticity was continuously monitored from 5 to 95°C every 0.5°C with an averaging time of 60 s. Protein concentrations were 0.34 mg/ml at pH 7.4 and 0.37 mg/ml at pH 4.8. The pathlength was 0.05 cm.

as insets to Fig. 4, *A* (pH7.4) and *B* (pH 4.8). At pH 7.4, $T_{1/2}$ for the β-sheet (217 nm) and random coil curves (202 nm) are 45.8 and 47.6°C, respectively. At pH 4.8, $T_{1/2}$ for the unfolding curves are higher than for pH 7.4, indicating an increase in thermal stability at pH 4.8 with $T_{1/2}$ for β-sheet at 50.4°C and for random coil at 51.4°C. We conclude that, at pH 4.8, MM-κI is more resistant to thermal unfolding than at pH 7.4. Van't Hoff analysis of the thermal unfolding curves at 217 nm (Fig. 4 *insets*) yielded midpoints (T_m) of 47.4 and 48.8°C. The effective enthalpies (ΔH_{vH}) were 119 and 159 kcal/mol at pH 7.4 and 4.8, respectively. These results are presented in the van't Hoff plot (Fig. 5) with data summarized in Table 1. The values of ΔH_{vH} at pH 7.4 and 4.8 (Table 1) are in agreement with those provided by calorimetry.

Near-UV CD is a sensitive tool for probing protein tertiary structure, since subtle perturbations in the environment of aromatic residues and disulfide bonds can lead to large changes in spectral shape and amplitude (Sears and Beychok, 1973; Woody, 1995). Thermal unfolding monitored at wavelengths specific for Trp, Tyr, and Phe side chains or for disulfide bonds provides information about tertiary structural stability and the presence of intermediates as a function of temperature and pH. Lack of coincidence in T_m for different wavelengths would support a multistate unfolding with intermediate states. The conformational stability of MM-κI (pH 7.4 and 4.8) was studied using near-UV CD to monitor temperature-dependent changes at wavelengths corresponding to the disulfide bonds and aromatic amino acids.

MM-κI contains two tryptophans (W35, W148), 10 tyrosines (Y32, Y36, Y49, Y86, Y87, Y91, Y140, Y173, Y186, Y192), eight phenylalanines (F62, F71, F73, F98, F116, F118, F139, F209), five cysteines, with four cysteines

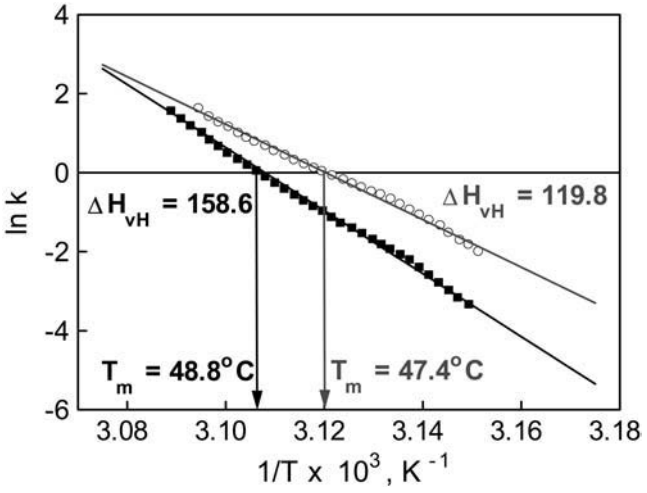

FIGURE 5 The van't Hoff analysis of MM-κI thermal unfolding in PBS. Data obtained at 217 nm, pH 7.4 (*circles*) and 4.8 (*squares*) were analyzed using methods described by Pace et al. (1989). Curves were constructed using linear least-squares fitting. Calculated values of ΔH_{vH} are presented in Table 1.

in two intrachain disulfide-bonds (Cys^{23}–Cys^{88}, Cys^{134}–Cys^{194}), and the fifth disulfide linked to Cys (Cys^{214}–Cys). Each domain contains a single tryptophan, W35 in the V_L and W148 in the C_L. Structural models of κI LCs position each tryptophan residue in the interior portion of its domain and are located very near to the intrachain disulfide bond (Amzel and Poljak, 1979). The signal from tryptophan may be significantly affected by close proximity to the disulfide bond.

The insets to Fig. 6 represent near-UV CD spectra of MM-κI recorded at 25°C before (indicated by *minus symbol*) and after (indicated by *asterisk symbol*) heating to 80°C at pH 7.4 (*A*) and pH 4.8 (*B*). At pH 7.4 (Fig. 6 *A*, *inset*) before heating, the spectrum is characterized by a broad peak with minimum at 265 nm and a shoulder at ~280 nm. After heating, a well-defined minimum is observed at 278 nm with the spectrum exhibiting an overall increase in magnitude. At pH 4.8 (Fig. 6 *B*, *inset*) before heating, maxima at 300 and 278 nm and a minimum at 292 nm are observed. After heating, the spectrum exhibits a broadened peak with reduced magnitude at 292 nm, a broad maximum at 265 nm, and no peaks at 300 and 278 nm. Comparison of these near-UV CD spectra at 25°C shows that the tertiary structure of MM-κI is dependent on pH. The spectra measured before (25°C) and after (25°*C) heating at each pH are different and indicate that heating irreversibly alters some of the native tertiary structural interactions of MM-κI. These observed differences prompted us to examine the temperature-dependent changes in ellipticity at specific wavelengths to probe specific environments of the disulfide bonds and various aromatic groups.

The thermal unfolding of MM-κI (pH 7.4 and pH 4.8) was monitored by near-UV CD at 260 nm for disulfide bonds and phenylalanine, at 280 nm for tyrosine, and at 290 and 295 nm for tryptophan. At pH 7.4 (Fig. 6 *A*), the T_m values for the curves at 260, 280, 290, and 295 nm are similar and range from 49.7 to 50.2°C. At pH 4.8 (Fig. 6 *B*), the T_m for the curves monitored at 280, 290, and 295 nm is 50.2°C, whereas that of the 260-nm curve is 72°C. This large 21.8°C difference in T_m indicates a non-two-state transition with the presence of structural intermediates and suggests that the disulfide bonds (which provide the largest contribution to CD at 260 nm) are significantly stabilized at pH 4.8 with respect to the rest of the molecule. Since structural models place the disulfide bonds and phenylalanines in the interior of each LC domain (Amzel and Poljak, 1979), the large increase in T_m at 260 nm observed at pH 4.8 suggests that the core of the protein undergoes heat-induced conformational changes at higher temperatures, thereby supporting the presence of unfolding intermediates. All CD measurements of thermal transition parameters were independent of protein concentration in the range explored (0.46–1.73 mg/ml), suggesting the absence of any large effects of protein aggregation on the transition parameters.

Far-UV CD was used to monitor the stability, unfolding cooperativity, and reversibility of MM-κI unfolding by

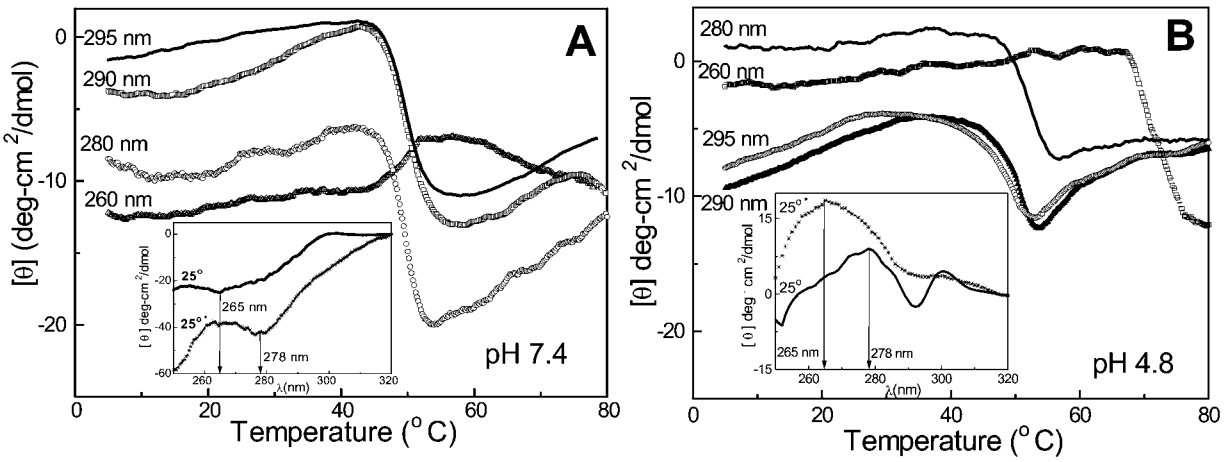

FIGURE 6 Near-UV CD data of MM-κI in PBS. Melting curves are shown at (*A*) pH 7.4 and (*B*) pH 4.8. Unfolding was monitored at 295 and 290 nm (tryptophan), 280 nm (tyrosine), and 260 nm (phenylalanine and disulfide bonds). Ellipticity was measured continuously from 5 to 80°C every 0.5°C with an averaging time of 90 s. Insets show near-UV CD spectra of MM-κI in PBS at pH 7.4 and pH 4.8 recorded at 25°C before (−) and after (*) heating to 80°C. At (*A inset*) pH 7.4, spectra (25°C), 19.2 mg/ml, 0.1 cm cell. Thermal unfolding (25°*C), 13.4 mg/ml, 0.2 cm cell. At (*B inset*) pH 4.8, spectra (25°C), 14.8 mg/ml, 0.1 cm cell. Thermal unfolding (25°*C), 14.8 mg/ml, 0.1 cm cell.

guanidine hydrochloride (GuHCl) at pH 7.4 and 4.8 (Fig. 7). Although a number of spectral types were observed, similar spectra were observed for specific ranges of GuHCl concentration. For clarity, a spectrum, showing the characteristic plot obtained for each secondary structural intermediate observed during denaturant-induced unfolding at pH 7.4 (*A*) and 4.8 (*B*), is presented. At pH 7.4 and 25°C, the spectra for MM-κI from 0 to 0.7 M GuHCl are similar. The spectrum for 0 M GuHCl is shown. A predominantly β-sheet native conformation is indicated by a negative minimum at 217 nm. At 0.8 M, the spectrum changes, with similar data being observed for samples dissolved in up to 1.0 M GuHCl. From 0.8 to 1.0 M GuHCl, the negative minimum is increased in magnitude and shifts from 217 nm to 212 nm, suggesting that, although the conformation is still predominantly β-sheet, the relative amount is reduced and the amount of random coil is increased. From 1.2 to 1.4 M GuHCl (1.4 M shown), a major conformational change occurs, indicating conversion of a large portion of β-sheet to random coil. Additional stages in the change from β-sheet to random coil are observed at 1.6 M, 1.8–2.0 M, and 2.2–2.8 M, with complete unfolding at 3 M and above that concentration. In addition, notable spectral changes are observed over the wavelength range from 235 to 215 nm at GuHCl

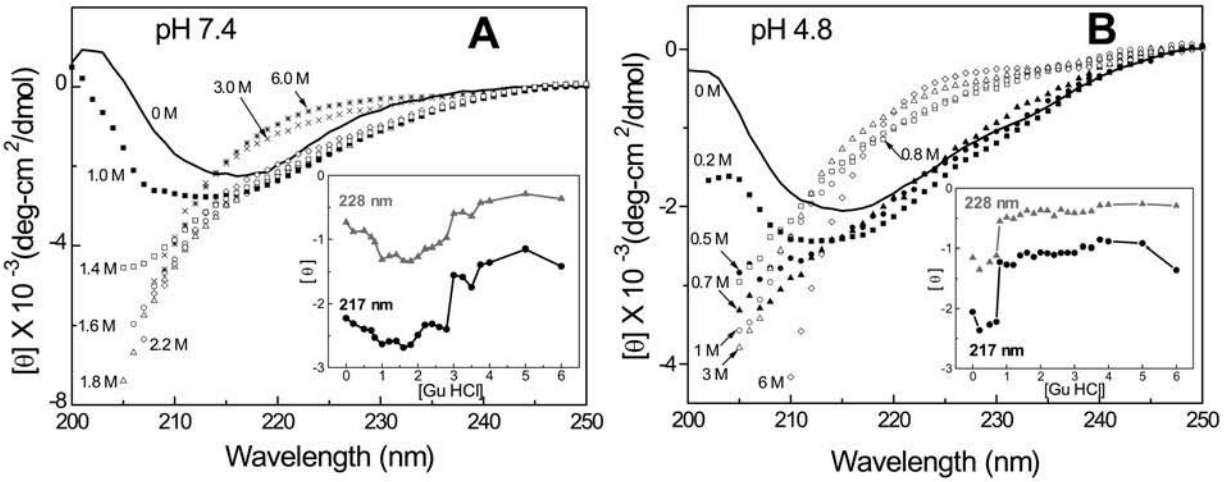

FIGURE 7 Far-UV CD spectra of MM-κI in PBS with increasing concentrations of GuHCl at (*A*) pH 7.4 and (*B*) pH 4.8. MM-κI, 0.4 mg/ml in PBS, and GuHCl (0, 0.2, 0.5, 0.7, 0.8, 1.0, 1.2, 1.4, 1.6, 1.8, 2.0, 2.2, 2.4, 2.6, 2.8, 3.0, 3.25, 3.5, 3.75, 4.0, 5.0, and 6.0 M) were incubated for at least 24 h at 25°C. Spectra were recorded at 25°C and each baseline was corrected for GuHCl at the same concentration as that recorded in the cell. Selected spectra representing the different spectral types and/or secondary structural contents are shown. Cell pathlength was 0.05 cm. Insets show ellipticity at 217 nm (*circles*) and 228 nm (*triangles*) as a function of GuHCl concentration for MM-κI at (*A*, *inset*) pH 7.4 and (*B*, *inset*) pH 4.8.

concentrations of 2.2 M and greater. The ellipticity is significantly reduced, providing evidence that complete unfolding from β-sheet to random coil has occurred. In contrast to thermally unfolded MM-κI, which retains a significant amount of secondary structure, the spectral shape and increased amplitude of the far-UV CD data of MM-κI at 1.8 M and higher GuHCl concentrations are consistent with a fully unfolded protein conformation. Thus, GuHCl-induced unfolding at pH 7.4 occurs in multiple stages that cannot be accounted for by independent unfolding of the two protein domains and therefore suggests the presence of conformational intermediates. In addition, chemical denaturation leads to a more extensive loss of secondary structure as compared to thermal denaturation. The reversibility of unfolding of MM-κI was studied at pH 7.4 by dilution of the protein from 1.4 M GuHCl to 0.5 M GuHCl. Superimposition of the spectrum of the dilution-refolded sample with that of the original 0.5 M GuHCl sample suggested that unfolding was completely reversible at pH 7.4 (data not shown).

The spectra of MM-κI at pH 4.8 in 0–6 M GuHCl at 25°C are shown in Fig. 7 *B*. At 0 M GuHCl, MM-κI exhibits a typical β-sheet spectrum similar to that at pH 7.4. At 0.2 M GuHCl, the significantly altered spectrum, with broadened minimum shifted to 209–213 nm and increased intensity, indicates that unfolding has begun and suggests that there is reduced stability toward denaturant at pH 4.8. Further spectral changes are observed at 0.5, 0.7, 0.8, and 1.0 M GuHCl, indicating a gradual β-sheet to random coil conversion upon increasing GuHCl concentration. Above 1.0 M GuHCl, the spectrum indicated that predominantly random coil was present and by 3.0 M, all β-sheet had been unfolded. The reversibility of unfolding of MM-κI at pH 4.8 was studied by dilution of the 1.4 M sample to 0.5 M GuHCl. The spectrum of the diluted sample was significantly different from that of the 0.5 M sample, indicating irreversibility of the GuHCl-induced unfolding of MM-κI at pH 4.8 (data not shown). Since GuHCl effectively prevents protein aggregation, this suggests that the irreversibility of the protein unfolding at pH 4.8 cannot be accounted for by increased protein aggregation at this pH. This is consistent with the thermal unfolding results, showing that the cooperativity ratio $\Delta H_{cal}/\Delta H_{vH}$ (which approximates the ratio of the molecular size to the size of the cooperatively unfolding unit) is lower at pH 4.8 than at pH 7.4—thereby suggesting that protein aggregation does not increase at low pH.

Molar ellipticity as a function of GuHCl concentration at pH 7.4 (Fig. 7 *A*, *inset*) and 4.8 (Fig. 7 *B*, *inset*) was examined. The GuHCl-induced changes in the β-sheets were monitored at 217 nm. The far-UV CD of the aromatic residues and disulfide bonds was monitored at 228 nm since spectral intensity at this wavelength is strongly dependent on the solvent composition (Sreerama et al., 1999; Khan et al., 1989). Due to the interior location of these groups, monitoring of the CD at 228 nm provides a method for probing the stability of the LC core. These plots show that unfolding of MM-κI at each pH occurs in multiple steps, and suggest that the chemical denaturation process involves unfolding intermediates. The concentration of GuHCl and the structural content of each intermediate are dependent on pH. At pH 4.8, unfolding begins and is completed at $<$1.0 M GuHCl, a much lower GuHCl concentration than at pH 7.4 (where MM-κI maintains a large amount of secondary structure up to ~3.0 M). This indicates that MM-κI is more susceptible to denaturant-induced unfolding at low pH, perhaps due to a less tightly packed surface that allows denaturant access to the LC core. The GuHCl-unfolding curves at pH 7.4 are not sigmoidal, suggesting the presence of secondary structural intermediates. At pH 4.8, the unfolding curves are less complex but still exhibit multiple stages. At 25°C, MM-κI exhibits markedly reduced stability at pH 4.8 in comparison to pH 7.4, as shown by the onset of unfolding at low GuHCl concentration.

The $\Delta G_{25°C}$ values derived from the unfolding curves at pH 7.4 are semiquantitative, i.e., the transitions exhibit multiple steps and cannot be interpreted as simple two-state (folded $\rightarrow$ unfolded) transitions. At pH 4.8, unfolding begins at the very low concentration of 0.2 M GuHCl, thereby precluding accurate definition of the pretransition baseline necessary for ΔG determination. Furthermore, GuHCl-induced unfolding at pH 4.8 is irreversible and accurate determination of ΔG is therefore not possible.

Analysis of the molar ellipticity (217 nm) in chemical denaturation curves (Fig. 7, *A* and *B*) yielded the values for apparent $\Delta G_{25°C}$ and $C_{1/2}$, which are listed in Table 1. For reasons mentioned previously, only the value for $C_{1/2}$ at pH 4.8 is presented. The value of apparent $\Delta G_{25°C}$ at pH 7.4 is similar to ΔG values reported for other LCs (Azuma et al., 1972; Tsunenaga et al., 1987; Wetzel, 1997) and is comparable or lower than the conformational stability of other globular proteins that ranges from 5 to 15 kcal/mol (Pfeil, 1981; Creighton, 1984).

The effect of pH on the secondary structure of MM-κI was studied in a series of titration experiments. Samples of MM-κI in PBS (pH 7.4) were titrated to acidic or basic pH and far-UV CD spectra were measured at 25°C (Fig. 8). Titration from pH 7.4 to 11.2 produced spectral changes, suggesting that MM-κI had partially unfolded from predominantly β-sheet at pH 7.4 to a mixture of β-sheet and random coil at pH 11.2 (Fig. 8 *A*). Spectra recorded after titration from pH 11.2 to 7.4 and 24 h incubation at 25°C showed base-induced unfolding to be partially reversible. Titration from pH 7.4 to 4 resulted in a partially unfolded MM-κI and titration from pH 7.4 to 1 led to more substantial unfolding (Fig. 8 *B*). Increasing the pH from either 4 or 1 to pH 7.4 with 24 h incubation at 25°C demonstrated irreversible acid-induced unfolding. Thus, MM-κI is predominantly β-sheet between pH 4.8 and 10, but becomes largely unfolded at more basic or more acidic pH values. Such pH-dependence suggests that

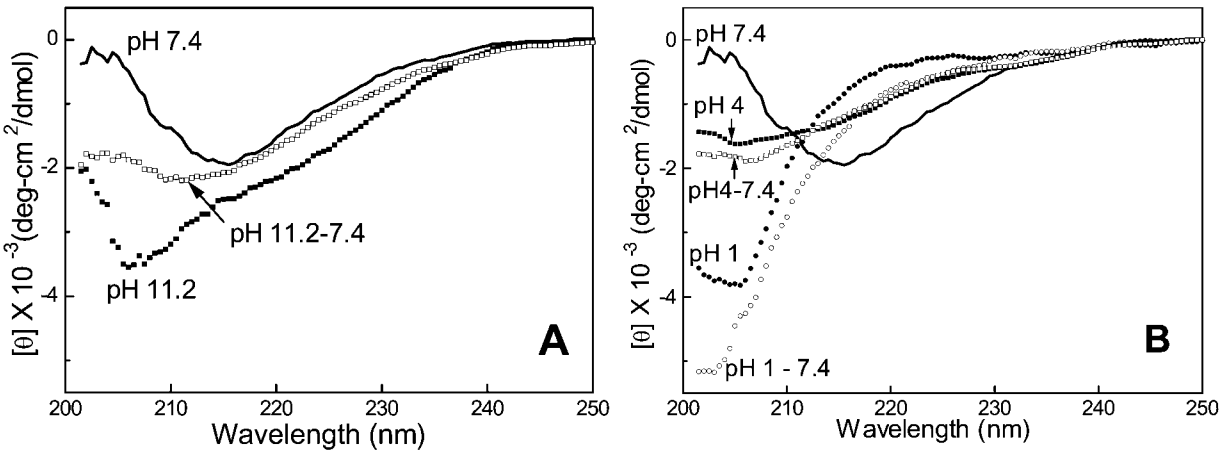

FIGURE 8 Far UV CD spectra of MM-κI pH titration. The protein concentration was 0.4 mg/ml and cell pathlength was 0.10 cm. (*A*) base: pH 7.4 (*solid line*); pH 11.2 (*solid squares*); pH 11.2 to pH 7.4 (*open squares*); (*B*) acid: pH 7.4 (*solid line*); pH 4 (*solid squares*); pH 4 to pH 7.4 (*open squares*); pH 1 (*solid circles*); pH 1 to pH 7.4 (*open circles*).

the protein conformation is significantly affected by the titration of acidic and basic side chains at extreme pH. In contrast, the change in protein stability observed between pH 7.4 and 4.8 may be linked to titration of the two His residues in the sequence of MM-κI. Base-induced unfolding is partially reversible, whereas acid-induced unfolding is not. This suggests that the pathways of base- and acid-induced unfolding of MM-κI are different. In addition, significant CD differences at 210–230 nm between the spectra recorded at pH 11.2 and 1 suggest different denatured states for acid- and base-induced unfolding.

In summary, the unfolding of native state MM-κI is a complex, multistep process that cannot be accounted for by the independent unfolding of the two protein domains. The final unfolded state of the protein is achieved through a number of intermediate states. The extent of the unfolding, and the unfolding pathway, depend on the type of denaturant (thermal or chemical), and distinct differences are observed at various pH values. Unfolding of MM-κI by GuHCl is largely reversible at pH 7.4, but is not reversible at pH 4.8. This suggests that, despite the conformational similarities of the native (predominantly β-sheet) and unfolded states (predominantly random coil), the unfolding pathways of MM-κI are different at each pH. The low $C_{1/2} = 0.75$ M GuHCl measured at pH 4.8 is similar to the values observed for other aggregation-prone LCs or their subdomains involved in such disorders as multiple myeloma, light chain deposition disease, and primary amyloidosis (Hurle et al., 1994; Wetzel, 1997; Wall et al., 1999). Thus, this environment-dependent instability may promote oligomerization of MM-κI in renal subcompartments where it may deposit in an insoluble pathologic form. The apparently low thermodynamic stability of the non-amyloidogenic MM-κI is comparable to that reported for amyloidogenic proteins, indicating that low thermodynamic stability is not sufficient for amyloid formation and suggesting that other (possibly kinetic) factors may be important. An understanding of the thermodynamic and kinetic properties of non-amyloidogenic myeloma LCs will provide a basis for comparison with the results of further studies on LCs that deposit as amyloid fibrils.

APPENDIX A: GLOSSARY

CD	Circular dichroism
DSC	Differential scanning calorimetry
ESI	Electrospray ionization
GuHCl	Guanidine hydrochloride
IEF	Isoelectric focusing
Ig LC	Immunoglobulin light chain
MALDI	Matrix-assisted laser desorption/ionization
MM-κI	Immunoglobulin light chain protein of the κI subtype isolated from the urine of an individual with multiple myeloma
MRW	Mean residue weight
MS	Mass spectrometry
PBS	Phosphate-buffered saline, 50 mM potassium phosphate, 0.15 M sodium chloride
SDS-PAGE	Sodium dodecyl sulfate polyacrylamide gel electrophoresis
$C_{1/2}$	Concentration of GuHCl at the midpoint of the denaturant unfolding transition, *M*
C_L	Constant domain of immunoglobulin light chain
$T_{1/2}$	Temperature at the midpoint of the transition
T_m	Melting temperature (corresponds to the maximum in the heat capacity function, $C_p(T)$, of the calorimetric transition), in °C
V_L	Variable domain of immunoglobulin light chain
ΔC_p	Heat capacity change between folded and thermally unfolded states
$\Delta G_{25°C}$	Free energy change of unfolding in the absence of GuHCl at 25°C, kcal/mol
ΔH_{cal}	Calorimetric enthalpy of unfolding, kcal/mol; $C_{p,max}$, maximum in the heat capacity function
ΔH_{vH}	Theoretical or van't Hoff enthalpy of unfolding, kcal/mol

The authors thank Ms. Cheryl A. England and Dr. Vickery Trinkaus-Randall for their tremendous assistance and support in the resubmission of this manuscript.

This work was supported with funds from an American Heart Association Medical Student Research Fellowship (C.M.C.), National Institutes of Health Predoctoral Training Grant No. T32 HL07291 (C.M.C. and J.D.C.), P01 HL26335, P01 HL68705 (L.H.C., A.L., C.E.C., M.S.), P41 RR10888 and S10 RR15942 (C.E.C.), R01 DK49596, M01 RR00750, (J.L., M.D.B.), the Gerry Foundation and the George Burr Jr. Amyloid Research Fund (M.T.W.).

REFERENCES

Amzel, L. M., and R. J. Poljak. 1979. Three-dimensional structure of immuno-globulins. *Annu. Rev. Biochem.* 48:961–997.

Azuma, T., K. Hamaguchi, and S. Migita. 1972. Denaturation of Bence Jones proteins by guanidine hydrochloride. *J. Biochem. (Tokyo).* 72:1457–1467.

Biltonen, R. L., and E. Freire. 1978. Thermodynamic characterization of conformational states of biological macromolecules using differential scanning calorimetry. *CRC Crit. Rev. Biochem.* 5:85–124.

Brandts, J. F., and L.-N. Lin. 1990. Study of strong to ultratight protein interactions using differential scanning calorimetry. *Biochemistry.* 29:6927–6940.

Brody, T. 1997. Multistep denaturation and hierarchy of disulfide bond cleavage of a monoclonal antibody. *Anal. Biochem.* 247:247–256.

Büchner, J., M. Renner, H. Lilie, H.-J. Hinz, R. Jaenicke, T. Kiefhaber, and R. Rudolph. 1991. Alternatively folded states of an immunoglobulin. *Biochemistry.* 30:6922–6929.

Chung, C. M., L. H. Connors, M. D. Benson, and M. T. Walsh. 2001. Biophysical analysis of normal transthyretin: implications for fibril formation in senile systemic amyloidosis. *Amyloid J. Protein Fold. Disorders.* 8:75–83.

Creighton, T. E. 1984. Proteins: Structures and Molecular Properties. W.H. Freeman, New York.

Dwulet, F. E., K. Strako, and M. D. Benson. 1985. Amino acid sequence of a λ VI primary (AL) amyloid protein (WLT). *Scand. J. Immunol.* 22:653–660.

Fasman, G. D. 1996. Circular Dichroism and the Conformational Analysis of Biomolecules. Plenum Press, New York.

Freire, E., and R. L. Biltonen. 1978. Statistical mechanical deconvolution of thermal transitions in macromolecules. I. Theory and application to biological systems: statistical mechanical deconvolution of thermal transitions in macromolecules. II. General treatment of cooperative phenomena. *Biopolymers.* 17:463–479, 481–496.

Fukada, H., J. M. Sturtevant, and F. A. Quiocho. 1983. Thermodynamics of the binding of L-arabinose and D-galactose to L-arabinose-binding protein of *E. coli*. *J. Biol. Chem.* 258:13193–13198.

Green, B. N., R. W. A. Oliver, A. M. Falick, C. H. Shackleton, E. Roitman, and H. E. Witkowska. 1990. Electrospray MS, LSIMS and MS/MS for the rapid detection and characterization of variant hemoglobins. *In* Biological Mass Spectrometry, A.L. Burlingame and J.A. McCloskey, editors. Elsevier, Amsterdam, The Netherlands. 129–145.

Greenfield, N., and G. D. Fasman. 1969. Computed circular dichroism spectra for the evaluation of protein conformation. *Biochemistry.* 8:4108–4116.

Hieter, P. A., E. E. Max, J. G. Seidman, J. V. Maizel, Jr., and P. Leder. 1980. Cloned human and mouse kappa immunoglobulin constant and J region genes conserve homology in functional segments. *Cell.* 22: 197–207.

Hurle, M. R., L. R. Helms, L. Li, W. Chan, and R. Wetzel. 1994. A role for destabilizing amino acid replacements in light-chain amyloidosis. *Proc. Natl. Acad. Sci. USA.* 91:5446–5450.

Khan, M. Y., G. Villaneuva, and S. A. Newman. 1989. On the origin of the positive band in the far-ultraviolet circular dichroic spectrum of fibronectin. *J. Biol. Chem.* 264:2139–2142.

Krishnan, K. S., and J. F. Brandts. 1978. Scanning calorimetry. *Methods Enzymol.* 49:3–14.

Laemmli, U. K. 1970. Cleavage of structural proteins during the assembly of the head of bacteriophage T4. *Nature.* 227:680–685.

Lim, A., J. Wally, M. T. Walsh, and C. E. Costello. 2001. Identification and location of a cysteinyl post-translational modification in an amyloidogenic kappa 1 light chain protein by electrospray ionization and matrix-assisted laser desorption/ionization mass spectrometry. *Anal. Biochem.* 295:45–56.

Loo, J. A., R. R. Loo-Ogorzalek, and P. C. Andrews. 1993. Primary to quaternary protein structure determination with electrospray ionization and magnetic sector mass spectrometry. *Organic Mass Spectr.* 28:1640–1649.

Lowry, O. H., N. J. Rosebrough, A. L. Farr, and R. J. Randall. 1951. Protein measurement with the Folin phenol reagent. *J. Biol. Chem.* 193:265–275.

Martsev, S. P., Z. I. Kravchuk, A. P. Vlasov, and G. V. Lyakhnovich. 1995. Thermodynamic and functional characterization of a stable IgG conformer obtained by renaturation from a partially structured low pH-induced state. *FEBS Lett.* 361:173–175.

Pace, C. N. 1986. Determination and analysis of urea and guanidine hydrochloride denaturation curves. *Methods Enzymol.* 131:266–280.

Pace, C. N., B. A. Shirley, and J. A. Thomson. 1989. Measuring the conformational stability of a protein. *In* Protein Structure: A Practical Approach. T.E. Creighton, editor. IRL Press, Oxford, UK. 311–330.

Pfeil, W. 1981. The problem of the stability of globular proteins. *Mol. Cell. Biochem.* 40:3–28.

Privalov, P. L., and N. N. Khechinashvili. 1974. A thermodynamic approach to the problem of stabilization of globular protein structure: a calorimetric study. *J. Mol. Biol.* 86:665–684.

Privalov, P. L., and S. A. Potehkin. 1986. Scanning microcalorimetry in studying temperature-induced changes in proteins. *Methods Enzymol.* 131:4–51.

Rigell, C. W., C. deSaussure, and E. Freire. 1985. Protein and lipid structural transitions in cytochrome c oxidase-DMPC reconstitutions. *Biochemistry.* 24:5638–5646.

Rowe, E. S., and C. Tanford. 1973. Equilibrium and kinetics of the denaturation of a homogeneous human immunoglobulin light chain. *Biochemistry.* 12:4822–4827.

Santoro, M. M., and D. W. Bolen. 1992. A test of the linear extrapolation of unfolding free energy changes over an extended denaturant concentration range. *Biochemistry.* 31:4901–4907.

Sears, D. W., and S. Beychok. 1973. Circular dichroism. *In* Physical Principles and Techniques of Protein Chemistry, Part C. S.J. Leach, editor. Academic Press, New York.

Shimba, N., H. Torigoe, H. Takahahi, K. Masuda, I. Shimada, Y. Arata, and A. Sarai. 1995. Comparative thermodynamic analyses of the Fv, Fab* and Fab fragments of anti-dansyl mouse monoclonal antibody. *FEBS Lett.* 360:247–250.

Sreerama, N., M. C. Manning, M. E. Powers, J.-X. Zhang, D. P. Goldenberg, and R. W. Woody. 1999. Tyrosine, phenylalanine, and disulfide contributions to the circular dichroism of proteins: circular dichroism spectra of wild-type and mutant bovine pancreatic trypsin inhibitor. *Biochemistry.* 38:10814–10822.

Sturtevant, J. M. 1987. Biochemical applications of differential scanning calorimetry. *Annu. Rev. Phys. Chem.* 38:463–488.

Tischenko, V. M., V. P. Zav'yalov, G. A. Medgyesi, S. A. Potehkin, and P. Privalov. 1982. A thermodynamic study of cooperative structures in rabbit immunoglobulin-G. *Eur. J. Biochem.* 126:517–521.

Towbin, H., T. Staehelin, and J. Gordon. 1979. Electrophoretic transfer of proteins from polyacrylamide gel and its preparative application. *Proc. Natl. Acad. Sci. USA.* 76:4350–4354.

Tsunenaga, M., Y. Goto, Y. Kawata, and K. Hamaguchi. 1987. Unfolding and refolding of a type κ immunoglobulin light chain and its variable and constant fragments. *Biochemistry.* 26:6044–6051.

Wall, J., M. Schell, C. Murphy, R. Hrncic, F. J. Stevens, and A. Solomon. 1999. Thermodynamic instability of human λ6 light chains: correlation with fibrillogenicity. *Biochemistry.* 38:14,101–14,108.

Wally, J., G. Kica, Y. Zhang, T. Ericsson, L. H. Connors, M. D. Benson, J. J. Liepnieks, J. Murray, M. Skinner, and R. L. Comenzo. 1999. Identification of a novel substitution in the constant region of a gene coding for an amyloidogenic κI light chain. *Biochim. Biophys. Acta.* 1454:49–56.

Walsh, M. T., and D. Atkinson. 1990. Calorimetric and spectroscopic investigation of the unfolding of human apolipoprotein *B*. *J. Lipid Res.* 31:1051–1062.

Walsh, M. T., H. Watzlawick, F. W. Putnam, K. Schmid, and R. Brossmer. 1990. The effect of the carbohydrate moiety on the secondary structure of β_2Glycoprotein I. *Biochemistry.* 29:6250–6257.

Wetzel, R. 1997. Domain stability of immunoglobulin light chain deposition disorders. *Adv. Protein Chem.* 50:183–243.

Woody, R. W. 1995. Circular dichroism. *Methods Enzymol.* 246:34–71.